JOC The Journal of Organic Chemistry

Featured Article

Cite This: J. Org. Chem. 2018, 83, 3034−3046

pubs.acs.org/joc

Samholides, Swinholide-Related Metabolites from a Marine Cyanobacterium cf. *Phormidium* sp.

Yiwen Tao,[†,∥,⊗] Pinglin Li,[‡,§,∥,⊗] Daojing Zhang,[∥,⊥] Evgenia Glukhov,[∥] Lena Gerwick,[∥] Chen Zhang,[∥] Thomas F. Murray,[#] and William H. Gerwick*[,∥,▽]

[†]Key Laboratory of Molecular Target & Clinical Pharmacology, School of Pharmaceutical Sciences and the Fifth Affiliated Hospital, Guangzhou Medical University, Guangzhou 511436, People's Republic of China

[‡]Key Laboratory of Marine Drugs, Chinese Ministry of Education, School of Medicine and Pharmacy, Ocean University of China, Qingdao 266003, People's Republic of China

[§]Laboratory for Marine Drugs and Bioproducts, Qingdao National Laboratory for Marine Science and Technology, Qingdao 266235, People's Republic of China

[∥]Center for Marine Biotechnology and Biomedicine, Scripps Institution of Oceanography, University of California San Diego, La Jolla, California 92093, United States

[⊥]State Key Laboratory of Bioreactor Engineering, East China University of Science & Technology, Shanghai 200237, People's Republic of China

[#]Department of Pharmacology, Creighton University School of Medicine, Omaha, Nebraska 68178, United States

[▽]Skaggs School of Pharmacy and Pharmaceutical Sciences, University of California San Diego, La Jolla, California 92093, United States

Supporting Information

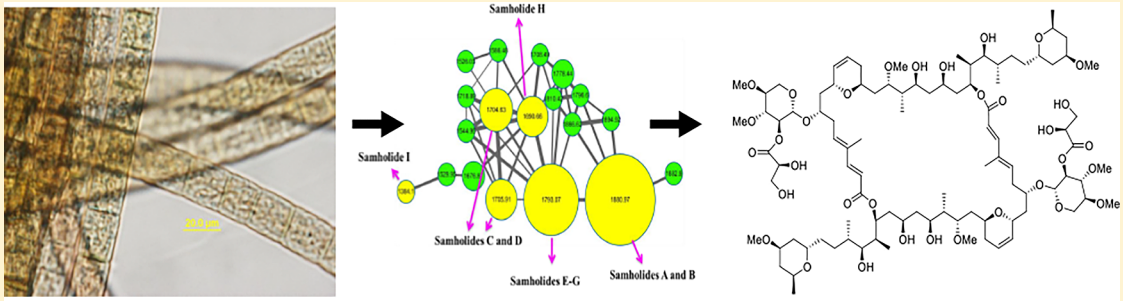

Cf. *Phormidium* sp. MS²-based Molecular Network Samholide A

ABSTRACT: Cancer cell cytotoxicity was used to guide the isolation of nine new swinholide-related compounds, named samholides A−I (**1**−**9**), from an American Samoan marine cyanobacterium cf. *Phormidium* sp. Their structures were determined by extensive analysis of 1D and 2D NMR spectroscopic data. The new compounds share an unusual 20-demethyl 44-membered lactone ring composed of two monomers, and they demonstrate structural diversity arising from geometric isomerization of double bonds, sugar units with unique glyceryl moieties and varied methylation patterns. All of the new samholides were potently active against the H-460 human lung cancer cell line with IC_{50} values ranging from 170 to 910 nM. The isolation of these new swinholide-related compounds from a marine cyanobacterium reinvigorates questions concerning the evolution and biosynthetic origin of these natural products.

INTRODUCTION

Cyanobacteria (blue-green alga) are a monophyletic bacterial phylum containing more than 60 genera with more than 400 species.[1] As a group, they are extraordinarily rich in structurally diverse and biologically active natural products.[2] Almost 500 new compounds have been isolated from cyanobacteria,[3] with peptides, polyketides, and hybrids thereof being the major representatives. Several of these natural products have inspired the development of new pharmaceutical agents, and 17 cyanobacterial-derived or inspired agents are in phase I or II drug development (in 2018) and are part of the global marine pharmaceutical clinical pipeline.[4]

The swinholides represent a family of macrolide natural products having a unique dimeric 44-membered or larger lactone ring. The first example was swinholide A, originally isolated by Kashman and Carmeli from the marine sponge *Theonella swinhoei* in 1985.[5] However, prior to this discovery, swinholide-type natural products had also been isolated from cultured cyanobacteria. Moore et al.[6] reported in 1977 a novel monomeric macrolide, tolytoxin, from the terrestrial cyanobacterium *Tolypothrix conglutinata* var. *colorata*

Received: January 4, 2018
Published: February 19, 2018

DOI: 10.1021/acs.joc.8b00028
J. Org. Chem. 2018, 83, 3034−3046

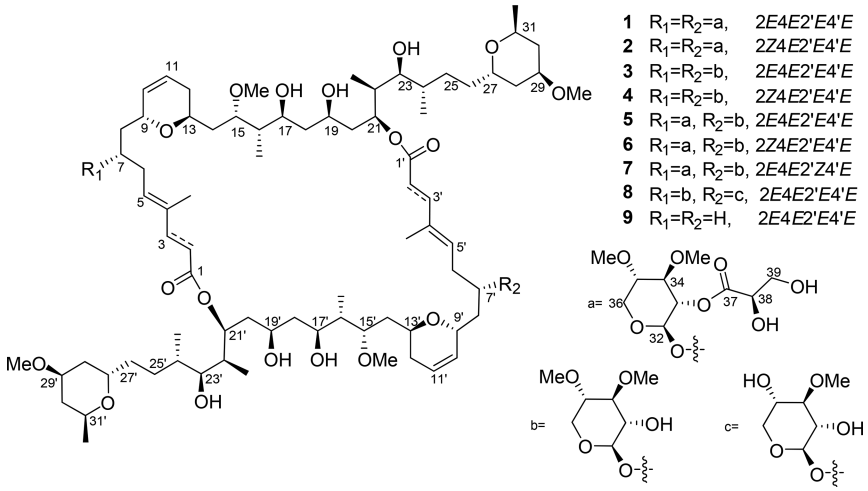

Figure 1. Structures of compounds **1**−**9**.

collected from Fanning Island. Tolytoxin showed potent cytotoxic and fungicidal properties and ultimately was found to possess a structure closely related to a monomeric half of swinholide A. In 1986, the same research group reported a series of tolytoxin-related macrolides, scytophycins A−E, from the cultured terrestrial cyanobacterium *Scytonema pseudohofmanni*.[7] The scytophycins were also structurally related to the swinholides and possessed potent cytotoxicity as well as broad-spectrum antifungal activity. In 2005, our laboratory reported two new glycosylated swinholides, ankaraholides A and B, from a Madagascar cyanobacterium of the genus *Geitlerinema* sp., together with swinholide A from a Fijian cyanobacterium *Symploca* cf. sp.[8]

To date, nearly 60 closely related swinholide-type compounds have been isolated from various species of mollusks, sea hares, nudibranchs, and red and brown algae, causing the true biosynthetic origin of this class of natural products to be confusing and ambiguous.[2,3,9−11] In some cases, it is relatively clear that these metabolites are produced by associated or preyed upon microorganisms (e.g., in the cases of macroalgae or mollusks, respectively). In the case of the sponge *Theonella* spp., because large numbers of cyanobacteria are present in the sponge tissue, it was hypothesized that the swinholides are cyanobacterial secondary metabolites.[9] However, Bewley et al. found that swinholide A was associated with a heterotrophic eubacterial fraction rather than the separated sponge and cyanobacterial cells.[10] Subsequently, Piel et al. sequenced the biosynthetic gene cluster for misakinolide A from a metagenomic sample of *Theonella* sp. along with its complement of symbionts.[11] Isolation of single filaments of the proposed bacterial source of the misakinolide cluster, *Entotheonella serta*, followed by multiple displacement amplification (MDA) and sequencing, confirmed that it was the source organism. Matrix-assisted laser desorption ionization (MALDI) imaging as well as catalyzed reporter deposition-fluorescence in situ hybridization (CARD-FISH) analysis provided additional support for this deduction. However, the same work provided highly analogous biosynthetic gene clusters from two cultured cyanobacteria, *Scytonema* sp. PCC 10023 and *Planktothrix paucivesiculata* PCC 9631, which produce scytophycin/tolytoxin and luminaolide, respectively. The gene sequencing studies of Piel et al. clearly revealed that two distinct phyla of microorganisms have the capacity to make this class of metabolite and likely reflect a complex set of vertical and horizontal evolutionary events.[11] Recently, a study of the antifungal constituents of two freshwater cyanobacteria, *Nostoc* sp. UHCC 0450 and *Anabaena* sp. strain UHCC 0451, revealed swinholide and scytophycin-type natural products, respectively.[12] Draft genomes of these two organisms revealed the presence of *trans*-AT biosynthetic gene clusters responsible for production of these molecules, and they were remarkably similar in sequence and architecture to those described by Piel for misakinolide A, scytophycin, and luminaolide. A phylogenetic analysis supported their origination through Horizontal Gene Transfer events.

As a class, the swinholides possess a number of significant bioactivities. Tolytoxin was found to inhibit the growth of a wide array of fungi with MIC values of 0.25−8 nM. It also showed strong cytotoxicity toward a variety of mammalian cells at similar IC_{50} values.[13] Scytophycins A and B displayed antiproliferative activity to the KB human nasopharyngeal carcinoma cell line with an IC_{50} of 1.2 nM. Other swinholide-related compounds have been found to have similar cytotoxicities with IC_{50} values in the low nanomolar to picomolar range.[14] The molecular target of the swinholides in mammalian cells has been determined to be actin, and at least some of these molecules exhibit nanomolar-potency binding characteristics at the same site of F-actin and G-actin. These potent biological features have thus inspired in-depth investigations of structurally diversified swinholide analogues.[15]

In the current study, nine new swinholide-type compounds, termed samholides A−I (**1**−**9**, Figure 1), were obtained from a field collection in American Samoa of the cyanobacterium cf. *Phormidium* sp. using a bioassay-guided isolation approach in combination with the MS^2-based molecular networking dereplication tool.[16] Their structures were determined by extensive analysis of 1D and 2D NMR spectra, and they share a unique 20-demethyl (compared with swinholide A) 44-membered lactone ring that is composed of two monomers. Structural variations among these new compounds result from differences in the methylation and esterification patterns decorating the sugars, as well as the double-bond geometries. Cytotoxicity was evaluated using the H-460 human lung carcinoma cell line and showed that all nine were potently active with IC_{50} values ranging from 170 to 910 nM. The variations in structure and attendant biological activities provide some initial structure−activity relationships (SAR) and reveal that the sugar units are important for high potency. Finally, their isolation from a marine cyanobacterium provides further evidence for cyanobacteria being a frequent and plentiful source of these actin-binding dimeric metabolites of the swinholide family.

DOI: 10.1021/acs.joc.8b00028
J. Org. Chem. 2018, 83, 3034−3046

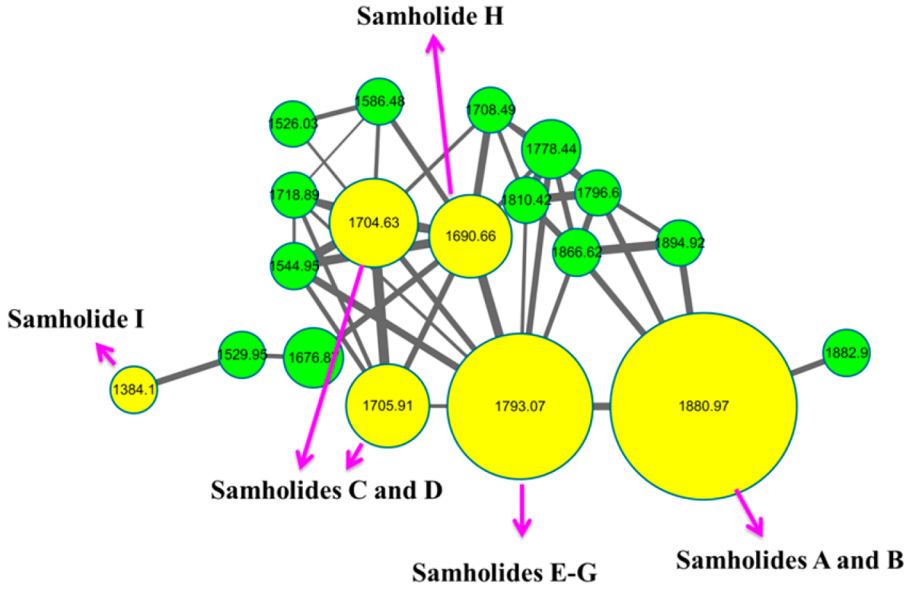

Figure 2. MS/MS-based molecular network of the samholides.[16] The cosine level was adjusted to 0.7. Nodes display measured masses of the molecular ions. The yellow nodes are samholide analogues that were isolated and defined in the current study, whereas the green nodes are potential samholide analogues not yet described due to the small amounts that were present. The size of the node is reflective of the relative amount of the indicated compounds.

RESULTS AND DISCUSSION

Tufts of a marine cyanobacterium, morphologically identified as cf. *Phormidium* sp., were collected at approximately 2 m water depth near American Samoa in July 2014. The preserved collection was repetitively extracted (2:1 CH_2Cl_2/MeOH) and fractionated using normal-phase vacuum liquid chromatography (VLC) to obtain nine fractions (Fr. A–I). Fractions and the crude extract were screened for cytotoxicity to H-460 human lung cancer cells at 1 and 10 μg/mL.[17] While several fractions showed cytotoxicity at the higher concentration, only the two most polar fractions (H, I) were active at 1 μg/mL. By contrast, the extract and all fractions were inactive in a neuromodulatory assay that evaluated the ability of these materials to modulate intracellular calcium mobilization.[18] LC–MS/MS molecular networking techniques revealed a distinct cluster of 19 nodes in fractions H and I (Figure 2 and p S104 in the Supporting Information), none of which matched any GNPS MS^2 library standards.[16] Reversed-phase HPLC of these two fractions yielded nine new compounds, given the names samholides A–I (**1**–**9**, Figure 1) to reflect their geographical origins, and these were collectively responsible for the potent cytotoxicity of these fractions.

Samholide A (**1**) gave a sodiated molecular ion peak by HRESIMS spectrum at m/z 1880.0657 $[M + Na]^+$ for a molecular formula of $C_{96}H_{160}O_{34}Na^+$ (calcd 1880.0683). However, the ^{13}C NMR (Table 1) of compound **1** showed only 48 distinct carbon signals, suggesting that **1** possessed a homodimeric structure. The ^1H NMR of samholide A displayed four doublet methyl resonances, each of which was composed of six protons for two symmetrical methyl groups at δ_H 0.83 (d, J = 7.02 Hz), 0.91 (d, J = 6.93 Hz), 0.98 (d, J = 6.74 Hz), and 1.20 (d, J = 6.18 Hz) as well as two overlapping symmetrical olefinic methyl signals at δ_H 1.80 (s). A cluster of oxygenated methines and methoxy groups was located between δ_H 3.10 and δ_H 5.00, and 10 olefinic protons appearing as 5 distinct signals were located between δ_H 5.67 to δ_H 7.61. Three olefinic signals, each composed of two isochronous protons, were deshielded to shifts of δ_H 5.78 (m), 6.34 (dd, J = 9.44, 3.17 Hz), and 7.61 (d, J = 15.54 Hz), indicating the presence of two trisubstituted, conjugated dienones. ^{13}C NMR analysis of compound **1** showed four ester carbonyls with two each at δ_C 170.7 and 170.64; the latter two reinforced the above assignments in that they were conjugated to two symmetrical dienes with carbon resonances at δ_C 153.1, 142.9, 123.3, and 113.5. There were also two symmetrical isolated double bonds at δ_C 133.9 and 129.7.

HSQC–TOCSY (Table 1) further enabled assignment of the ^1H and ^{13}C NMR data to two symmetrical pentose units with anomeric carbons at δ_C 102.1 and four oxygenated carbons each at δ_C 82.4, 73.2, 79.3, and 62.3. These NMR data were generally indicative of a swinholide-related polyketide structure possessing a sugar unit, and thus was of a structure class related to that of ankaraholide A which had been previously isolated from another cyanobacterium, *Geitlerinema* sp. collected in Madagascar.[8]

The main differences in the NMR data between compound **1** and ankaraholide A were between C-16 and C-22, and C2 and C5, which nevertheless showed highly similar $\Delta\delta$-values ranging from 0.8 to 1.4 ppm, relative to the average of 0.3 ppm for the remainder of the comparable carbon signals (Table S1, Supporting Information). Considering the variability of the methyl groups at C-16 and C-20 in the known swinholides,[3] these differences between **1** and ankaraholide suggested that it might possess the uncommon 16-methyl-20-demethyl skeleton, a carbon framework only previously appearing in the partial monomer structure of swinholide G.[18] This speculation was supported by HMBC analysis that revealed that the long-range correlations from the methyl groups at C-16 and C-22 formed two distinct and nonoverlapping spin networks. Confirmation of this framework was obtained by COSY, HMBC, and HSQC-TOCSY experiments (Table 1 and Figures S9–S13, Supporting Information) which outlined a linear spin system decorated with secondary methyl and oxymethine groups and yielded a homodimeric structure possessing a 20,20′-didemethylswinholide A skeleton (Figure 3). Three additional carbon signals were observed in **1** compared to ankaraholide A and included one ester carbonyl group at δ_C 170.7, one oxygenated methine at

DOI: 10.1021/acs.joc.8b00028
J. Org. Chem. 2018, 83, 3034–3046

Table 1. NMR Data for Compound 1 in $CDCl_3$ at 600 MHz (^1H)[a] and 125 MHz (^{13}C)[b], Respectively

	^{13}C	^1H	COSY	HMBC	HSQC-TOCSY	ROESY
1/1′	170.6					
2,2′	113.5	5.78 (overlapped)	3/3′	3/3′, 1/1′	2/2′, 3/3′	4/4′-Me
3,3′	153.1	7.6 d (15.5)	2/2′	2/2′, 4/4′, 4/4′-Me, 5/5′	2/2′, 3/3′	2/2′, 5/5′, 15/15′, 38/38′-OH, 39/39′-OH
4/4′	133.9					
4,4′-Me	12.1	1.74 s	5/5′	3,4,5	4/4′-Me, 5/5′	2/2′, 6/6′, 8/8′
5,5′	142.9	6.34 dd (9.44, 3.17)	6/6′, 4/4′-Me	4/4′-Me, 3/3′, 6/6′, 7/7′	4/4′-Me, 5/5′, 6/6′, 7/7′, 8/8′, 9/9′	3/3′, 7/7′, 39/39′-OH
6,6′	33.5	2.50 d (12.76) 2.37 m	5/5′, 7/7′	4/4′, 5/5′, 7/7′	4/4′-Me, 5/5′, 6/6′, 7/7′, 8/8′, 9/9′	4/4′-Me, 8/8′, 9/9′, 10/10′
7,7′	79.0	4.10 m	6/6′, 8/8′	5/5′, 6/6′, 32/32′	5/5′, 6/6′, 7/7′, 8/8′, 9/9′	5/5′, 32/32′
8,8′	39.9	2.33 m 1.53 m	7/7′, 9/9′	6/6′, 7/7′, 9/9′, 10/10′	5/5′, 6/6′, 7/7′, 8/8′, 9/9′	4/4′-Me, 13/13′
9,9′	68.7	4.21 d (11.81)	8/8′, 10/10′	8/8′, 10/10′, 11/11′, 13/13′	5/5′, 6/6′, 7/7′, 8/8′, 9/9′, 10/10′, 11/11′, 12/12′	6*a*/6a′, 14/14′
10,10′	129.7	5.68 d (10.26)	9/9′, 11/11′, 12/12′	9/9′, 12/12′	8/8′, 9/9′, 10/10′, 11/11′, 12/12′, 13/13′, 14/14′	8/8′
11,11′	123.3	5.77 m	10/10′, 12/12′	9/9′, 12/12′, 13/13′	8/8′, 9/9′, 10/10′, 11/11′, 12/12′, 13/13′, 14/14′	
12,12′	31.5	2.08 d (17.58) 1.96 m	11/11′, 13/13′	10/10′, 11/11′, 13/13′, 14/14′	7/7′, 10/10′, 11/11′, 12/12′, 13/13′, 14/14′	
13,13′	63.4	3.69 m	12/12′, 14/14′a		12/12′, 13/13′, 14/14′, 15/15′	8*a*/8a′
14,14′	36.4	1.86 m 1.64 m	13/13′, 15/15′	13/13′, 15/15′, 16/16′	12/12′, 13/13′, 14/14′, 15/15′	
15,15′	75.0	4.07 m	14/14′	14/14′, 15/15′-OMe, 16/16′-Me, 16/16′, 17/17′	12/12′, 13/13′, 14/14′, 15/15′	6*a*/6a′, 5/5′, 17/17′−OH
16,16′	41.2	1.59 m	16/16′-Me, 15/15′	16/16′-Me, 18/18′	13/13′, 14/14′, 15/15′, 16/16′, 16,16′-Me	
16,16′-Me	9.3	0.83 d (6.85)	16/16′	15,16,17	16,16′-Me, 16/16′, 17/17′, 18/18′, 19/19′	
17,17′	73.5	3.84 t (9.5)	18/18′	15/15′, 16/16′-Me, 16/16′, 18/18′, 19/19′	16/16′-Me, 18/18′, 17/17′, 19/19′	16/16′-Me
18,18′	41.4	1.76 m		17/17′, 19/19′	17/17′, 18/18′, 19/19′, 20/20′	
19,19′	69.6	3.95 m			18/18′, 19/19′, 20/20′, 21/21′	17/17′-OH
20,20′	42.1	1.94 m 1.52 m		21/21′,	20/20′, 21/21′, 19/19′	
21,21′	70.3	5.84 d (11.37)	20/20′	1′/1′, 19/19′, 23/23′, 20/20′, 22/22′, 22/22′-Me	19/19′, 20/20′	23/23′, 23/23′-OH, 39/39′-OH, 38/38′-OH
22,22′	40.5	1.65 m		22/22′-Me, 23/23′	22,22′-Me, 22/22′, 23/23′, 24/24′,25/25′, 26/26′	
22,22′-Me	9.7	0.90 d (6.85)	22/22′	21,22,23	22,22′-Me, 22/22′, 23/23′	
23,23′	75.8	3.18 d (9.01)	22/22′, 24/24′	21/21′, 22/22′, 24/24′-Me, 25/25′	22/22′-Me, 22/22′, 23/23′	21/21′, 22/22′-Me, 24/24′-Me
24,24′	33.4	1.65 m		23/23′, 26/26′	22/22′, 23/23′, 24/24′-Me, 24/24′, 25/25′, 26/26′	
24,24′-Me	17.2	0.95 d (6.67)	24/24′	23,24,25	24,24′-Me, 24/24′, 25/25′, 26/26′, 27/27′	
25,25′	23.2	1.22 m		26/26′,	24,24′-Me, 24/24′, 25/25′, 26/26′, 27/27′	
26,26′	29.3	1.80 m 1.22 m		25/25′, 27/27′,	24/24′-Me, 25/25′, 26/26′, 27/27′	
27,27′	71.5	3.94 m		29/29′, 31/31′	24/24′-Me, 25/25′, 26/26′, 28/28′, 29/29′, 30/30′	
28,28′	35.1	1.77 m 1.55 m		29/29′, 30/30′	27/27′, 28/28′, 29/29′, 31/31′, 30/30′	
29,29′	73.5	3.50 m		28/28′, 31/31′	28/28′, 29/29′, 30/30′, 31/31′, 31/31′-Me,	
30,30′	38.9	1.94 m 1.15 m		29/29′	28/28′, 29/29′, 30/30′, 31/31′, 31/31′-Me	
31,31′	64.7	3.64 m	31/31′-Me	27/27′, 29/29′, 31/31′-Me	28/28′, 29/29′, 30/30′, 31/31′, 31/31′-Me	
31,31′-Me	21.9	1.16 d (6.19)	31/31′	30,31	28/28′, 29/29′, 30/30′, 31/31′, 31,31′-Me	
32,32′	102.1	4.78 d (6.09)		7/7′, 33/33′, 36/36′	32/32′, 33/33′, 34/34′, 35/35′, 36/36′	5/5′, 7/7′, 34/34′
33,33′	73.5	4.76 dd (8.21, 6.29)	34/34′	32/32′, 34/34′, 37/37′	32/32′, 33/33′, 34/34′, 35/35′, 36/36′	34/34′-OMe, 35/35′
34,34′	82.4	3.25 t (7.50)	33/33′	33/33′, 34/34′-OMe, 35/35′	32/32′, 33/33′, 34/34′, 35/35′, 36/36′	32/32′
35,35′	79.3	3.33 m			32/32′, 33/33′, 34/34′, 35/35′, 36/36′	33/33′

DOI: 10.1021/acs.joc.8b00028
J. Org. Chem. 2018, 83, 3034−3046

Table 1. continued

36,36′	62.3	4.00 dd (14.79, 7.83) 3.30 m	35/35′	32/32′, 34/34′, 35/35′-OMe	32/32′, 33/33′, 34/34′, 35/35′, 36/36′	
37/37′	170.7					
38,38′	72.4	4.06 m	38/38′−OH, 39/39′	37/37′, 39/39′	38/38′, 39/39′	3/3′
39,39′	64.7	3.70 m 3.50 m	38/38′, 39/39′−OH	38/38′	38/38′, 39/39′	24/24′-Me
15,15′-OMe	57.5	3.37 s		15/15′	15,15′-OMe	
29,29′-OMe	55.4	3.32 s		29/29′	29,29′-OMe	
34,34′-OMe	60.1	3.45 s		34/34′	34,34′-OMe	
35,35′-OMe	58.3	3.42 s		35/35′	35,35′-OMe	
17,17′−OH		4.82 s		17/17′	16/16′-Me, 17/17′, 18/18′	
19/19′-OH		5.77 m	19/19′		19/19′, 18/18′	
23,23′-OH		4.64 br s	23/23′	22/22′	22/22′-Me, 22/22′, 23/23′, 31/31′	21/21′, 24/24′-Me, 31/31′
38,38′-OH		5.03 d (3.00)	38/38′	37/37′, 38/38′, 39/39′	38/38′, 39/39′	2/2′, 3/3′, 21/21′
39,39′-OH		4.81 br s	39/39′		38/38′, 39/39′	3/3′, 5/5′, 21/21′

[a]^{1}H and 2D NMR spectra were run on a Bruker Advance III DRX-600 MHz NMR spectrometer. [b]^{13}C NMR spectra were run on a Varian X-Sens 500 MHz NMR spectrometer (125 MHz).

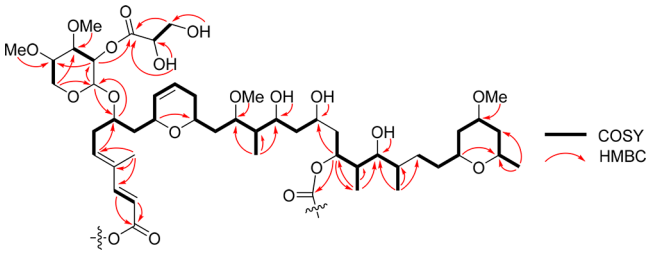

Figure 3. Key COSY and HMBC correlations of the monomeric structure present in samholide A (**1**).

δ_C 72.4, and one oxygenated methylene at δ_C 64.7. HMBC and COSY data clarified that these latter resonances and their associated protons were connected and formed a glyceric acid moiety. A neutral fragment ion loss of m/z 88 was observed in the MS/MS spectrum of **1**, supporting the nature of this substituent.

While the spin system of H-32 to H-36 for a pentapyranose sugar was apparent in compound **1**, H-32 and H-33 were overlapped and thus introduced a degree of uncertainty. However, this was resolved by consideration of the HMBC network between these proton and carbon atoms (Table 1 and Figure 3). Moreover, this spin connectivity between H-32/H-33/H-34/H-35/H_2-36 was directly observed in the COSY spectrum of compound **3** (Table 2). The large vicinal diaxial coupling constants between H-32, H-33, H-34, H-35, and Ha-36 (all between 6 and 9 Hz, Table 1) in **1** were indicative of the β-xylopyranoside unit, and this was further confirmed by ROESY correlations between H-32 and H-34 and Ha-36 (Figure 4 and Figures S14 and S15). These xylose units were attached to C-7/7′ on the basis of reciprocal HMBC correlations between H-7/7′ and C-32/32′ and H32/32′ and C-7/7′. HMBC correlations between two OMe resonances at δ_H 3.45 and 3.42 with carbons at δ_C 82.4 and 79.3 were indicative of two di-*O*-methylxylopyranoside units, and by consideration of the ^{13}C NMR assignments for this sugar (Table 1), these could be placed at C-34 and C-35. The glyceric acid moiety was connected through the oxygen atom at C-33 by HMBC correlation of H-33 with C-37.

All known swinholide-type compounds, irrespective of origin (sponge, cyanobacteria, algae, nudibranch), possess a highly analogous monomeric carbon skeleton as well as stereoconfigurations at comparable chiral centers (Figure 5); this latter aspect has been confirmed in two cases by X-ray crystallographic analysis[7,9] as well as via total synthesis.[19−21] As a result, it has been proposed that these swinholide-type metabolites are produced by highly similar polyketide synthase-type biosynthetic gene clusters.[11] In the present case, similarities between the ^{1}H and ^{13}C NMR chemical shifts and coupling constants of the protons at the chiral centers of compound **1** and those of previously reported swinholides, as well as the ankaraholides, strongly suggest that they have the same configurations at comparable centers (Table 1 and Tables S1 and S2, Supporting Information).[7,8] With the relative configuration of the sugar units defined as above from coupling constant analysis, these could be related to the aglycone stereoconfiguration by several ROESY correlations. ROESY correlations of H-32/H-7 (H-32′/H-7′), 39-OH/H-5 (39′-OH/H-5′), 39-OH/H-3 (39′-OH/H-3′), 38-OH/H-2 (38′-OH/H-2′), 38-OH/H-21′ (38′-OH/H-21), and 38-OH/H-3 (38′-OH/H-3′), in combination with molecular modeling, revealed that the sugar unit must be of L configuration (Figure 4). The configuration at C-38 (C-38′) was not discernible from these data, but given that all occurrences of glyceric acid in 26 cyanobacterial natural products are 2*R*, we predict samholide A to possess 38*R* (38′*R*) stereochemistry as well. Indeed, the glyceric acid unit configuration was rigorously established as D by chiral HPLC analysis of the acid hydrolysate of compound **5** in comparison with authentic standards. The geometry of the C-2-C-3 and C-4-C-5 double bonds were determined to both be *E*, the former by a characteristic 15.6 Hz *J* value between H-2 and H-3, and the latter from ROESY correlations between H-2 and the C-4 methyl group, H-3 and H-5, and H_2-6 and the C-4 methyl group (Figure 4). Thus, both the constitutive and stereostructure of samholide A (**1**) was established.

The molecular formula of samholide B (**2**) was identical to that of compound **1** by HRESIMS, and it had a very similar profile of ^{1}H and ^{13}C NMR shifts as well (Table 2 and 3). The main difference in the ^{1}H NMR of **2** was a different pattern of olefinic protons, including one that integrated for a single proton and was quite distinct from those in samholide A [δ_H 6.51 (d, J = 12.6 Hz)]. Moreover, the C-4 and C-4′ vinyl methyl groups were present as two distinct signals, and a number of other resonances appeared "twinned". These data, along with a second proton ascribed to H-2′ that had the same large *trans*-type coupling as present in **1** ($J_{H2'/H3'}$ = 15.6 Hz), along with ROESY correlations between H-2/H-3, H3/H-5, H-2′/4′-Me, and H-3′/H-5′, indicated that compound **2** was the C-2 double bond isomer of **1** with an overall heterodimeric structure.

DOI: 10.1021/acs.joc.8b00028
J. Org. Chem. 2018, 83, 3034−3046

Table 2. ^{1}H NMR Data for Compounds 2−9 in $CDCl_3$ at 600 MHz

	2		3	4		5		6		7		8[a]		9
	δ_H	$\delta_{H'}$	$\delta_H/\delta_{H'}$	δ_H	$\delta_{H'}$	δ_H	$\delta_{H'}$	δ_H	$\delta_{H'}$	δ_H	$\delta_{H'}$	δ_H	$\delta_{H'}$	$\delta_H/\delta_{H'}$
2,2′	5.79 m	5.67 m	5.79 d (15.59)	5.69 m	5.82 m	5.79 d (15.48)		5.68 d (12.47)	5.81 d (15.68)	5.80 m	5.66 d (12.72)	5.80 d (15.6)		5.80 d (15.62)
3,3′	6.51 (d (12.6)	7.50 d (15.6)	7.53 (d 15.56)	6.46 d (12.41)	7.39 d (15.56)	7.57 d (15.55)	7.52 d (15.56)	6.52 d (12.62)	7.44 d (15.54)	7.47 d (15.63)	6.46 d (12.69)	7.55 d (15.6)		7.47 d (15.62)
4,4′-Me	1.86 s	1.77 s	1.82 s	1.84 s	1.82 s	1.75 s	1.82 s	1.86 s	1.81 s	1.78 s	1.86 s	1.83 s		1.80 s
5,5′	5.84 dd (7.06, 6.27)	6.1 dd, (6.53, 6.40)	6.31 dd (7.55, 7.37)	5.98 t (6.33)	6.09 t (6.23)	6.33 m	6.32 m	5.86 t (7.00)	6.14 t (6.87)	6.11 t (6.88)	5.97 br s	6.35 m		6.19 t (7.03)
6,6′	2.55 dd (14.73, 5.62)	2.62 br d (13.34)	2.59 ddd (2.85, 6.14, 14.47)	2.56 m	2.64 m	2.50 d (13.39)	2.67 d (12.99)	2.57 ddd (4.06, 6.48, 13.87)	2.69 ddd (4.38, 6.03, 11.73)	2.59 m	2.57 m	2.60 m		2.47 ddd (3.24, 7.14, 14.94)
	2.38 m	2.28 m	2.37 dt (8.86, 14.34)	2.34 m	2.36 m	2.35 m	2.35 m	2.40 dt (7.02, 15.36)	2.28 dt (7.45, 15.12)	2.34 m	2.41 dt (7.38, 14.56)	2.38 m		2.31 dt (7.56, 15.19)
7,7′	4.06 m		4.04 m	4.01 m		4.02 m	3.99 m	3.97 m	4.00 m	4.03 m	3.97 m	4.08 m		4.04 ddd (4.25, 7.90, 11.76)
8,8′	2.28 m		2.25 ddd (5.02, 9.81, 15.0)	2.10 m		2.29 m		2.10 m	2.10 m	2.19 m	2.05 m	2.26 m		1.89 m
	1.54 m		1.63 m	1.64 m		1.67 m		1.55 m	1.67 m	1.54 m	1.64 m	1.62 m		1.52 m
9,9′	4.30 m		4.30 m	4.36 m		4.21 d (11.37)	4.31 brs	4.29 m	4.39 m	4.28 m	4.38 m	4.29 m		4.34 d (10.74)
10,10′	5.70 m		5.74 m	5.74 m		5.72 m	5.78 m	5.69 m	5.78 m	5.71 m		5.74 m		5.65 m
11,11′	5.80 m		5.74 m	5.80 m		5.80 m	5.71 m	5.80 m	5.69 m	5.74 m		5.77 m		5.81 m
12,12′	2.01 m		1.97 m	1.96 m		2.08 d (17.61)		1.97 m		1.95 m		1.97 m		1.98 m
						1.98 m								
13,13′	3.67 m		3.63 m	3.64 m		3.69 m		3.68 m		3.79 m		3.64 m		3.68 m
14,14′	1.87 m		1.78 m	1.87 m		1.84 m		1.88 m		1.84 m		1.77 m		1.86 m
	1.62 m		1.64 m	1.55 m		1.63 m		1.56 m		1.58 m		1.64 m		1.59 m
15,15′	4.06 m		4.01 m	3.78 m		4.05 m		3.78 m[a]	3.82 m[a]	3.82 m		4.08 m		3.83 m
16,16′	1.54 m		1.51 m	1.55 m		1.59 m		1.65 m		1.63 m		1.66 m		1.68 m
16,16′-Me	0.81 d (6.0)	0.82 d (6.0)	0.78 d (6.98)	0.83 d (6.54)	0.84 d (6.32)	0.80 d (7.14)	0.78 d (7.02)	0.82 d (6.91)	0.81 d (7.13)	0.83 d (7.13)	0.84 d (7.75)	0.79 d (6.36)	0.78 d (6.35)	0.83 d (7.02)
17,17′	3.85 m		3.84 t (9.70)	3.80 m		3.88 m		3.76 m		3.86 m		3.85 m		3.84 m
18,18′	1.76 m		1.70 m	1.79 m		1.74 m		1.70 m		1.85 m		1.72 m		1.87 m
	1.63 m		1.41 m	1.41 m		1.55 m		1.55 m		1.50 m		1.41 m		1.50 m
19,19′	3.93 m	3.88, m	3.88 t, (10.55)	3.85 m	3.79 m	3.99 m	3.88 m	3.88 m		3.87 m	3.85 m	3.90 m		3.84 m
20,20′	1.94 m		1.87 t (12.35)	1.87 m		1.90 m		1.87 m		1.87 m		1.85 m		1.89 m
	1.53 m		1.52 m	1.53 m		1.55 m		1.53 m		1.57 m		1.53 m		1.55 m
21,21′	5.63 d (9.82)	5.71 m	5.56 d (11.09)	5.64 m	5.66 m	5.71 m		5.60 d (10.39)	5.63 d (10.00)	5.65 m	5.69 m	5.55 d (11.17)		5.65 m
22,22′	1.64 m		1.65 m	1.64 m		1.69 m		1.76 m		1.73 m		1.76 m		1.74 m
22,22′-Me	0.87 d (6.81)	0.89 d (6.86)	0.90 d (6.89)	0.87 d (8.45)	0.89 d (7.47)	0.91 d (6.92)	0.89 d (7.13)	0.89 d (6.78)	0.88 d (6.78)	0.86 d (7.03)	0.90 d (6.95)	0.91 m		0.91 d (6.93)
23,23′	3.17 d (9.69)	3.12 d (9.59)	3.19 m	3.09 m		3.20 m		3.15 d (9.39)	3.12 d (9.83)	3.12 m		3.20 m		3.14 dd (1.52, 9.66)
24,24′	1.67 m		1.68 m	1.69 m		1.69 m		1.68 m		1.66 m		1.68 m		1.66 m
24,24′-Me	0.97 d (7.15)	0.95 d (7.07)	0.93 d (6.73)	0.97 d (6.10)		0.96 d (7.17)	0.95 d (7.23)	0.98 d(6.80)	0.96 d (6.74)	0.97 d (6.18)	0.96 d (6.3)	0.93 m		0.98 d (6.74)
25,25″	1.25 m		1.34 m	1.37 m		1.35 m		1.39 m		1.35 m		1.36 m		1.37 m

DOI: 10.1021/acs.joc.8b00028
J. Org. Chem. 2018, 83, 3034−3046

Table 2. continued

	2		3	4		5		6		7		8[a]		9
	δ_H	$\delta_{H'}$	$\delta_H/\delta_{H'}$	δ_H	$\delta_{H'}$	δ_H	$\delta_{H'}$	δ_H	$\delta_{H'}$	δ_H	$\delta_{H'}$	δ_H	$\delta_{H'}$	$\delta_H/\delta_{H'}$
			1.17 m	1.25 m		1.20 m		1.24 m		1.24 m		1.21 m		1.23 m
26,26′	1.88 m		1.83 m	1.86 m		1.86 m		1.87 m		1.86 m		1.84 m		1.87 m
	1.25 m		1.26 m	1.25 m		1.27 m		1.25 m		1.22 m		1.26 m		1.24 m
27,27′	3.99 m		3.98 m	3.98 m		3.98 m		3.99 m		3.97 m		3.97 m		3.98 m
28,28′	1.82 m		1.79 m	1.82 m		1.81 m		1.82 m		1.80 m		1.79 m		1.81 m
	1.59 m		1.59	1.56 m		1.59 m		1.58 m		1.57 m		1.58 m		1.58 m
29,29′	3.53 m		3.52 ddd 4.4, (9.83, 14.17)	3.52 m		3.52 m		3.52 m		3.52 m		3.52 m		3.52 m
30,30′	1.99 m		1.95 m	1.97 m		1.98 m		1.99 m		1.94 m		1.97 m		1.98 m
	1.18 m		1.18 m	1.16 m		1.19 m		1.18 m		1.17 m		1.17 m		1.16 m
31,31′	3.67 m		3.69 dddd (2.88, 6.13, 12.0, 15.0)	3.68 m		3.69 m		3.69 m		3.67 m		3.70 m		3.69 m
31,31′-Me	1.18 d (6.36)	1.17 d (6.14)	1.20 d (6.18)	1.20 d (5.9)		1.17 d (5.90)	1.19 d (6.44)	1.19d (6.25)		1.18 d (6.24)	1.20 d (6.3)	1.21 d (6.6)		1.20 d (6.18)
32,32′	4.67 d (6.91)	4.74 d (6.80)	4.43 d (6.64)	4.39 m	4.46 d (6.6)	4.81 d (4.98)	4.46 d (5.45)	4.65 d (6.77)	4.39 d (6.72)	4.71 m	4.43 d (6.29)	4.47 d (6.69)	4.53 d (5.45)	
33,33′	4.82 (dd, 8.33, 7.02)		3.28 t 7.15	3.29 m		4.74 t 6.11	3.27 m	4.83 dd (6.85, 8.39)	3.52 m	4.83 dd (7.18, 8.13)	3.37 m	3.40 m	3.36 m	
34,34′	3.34 m		3.24 m	3.20 m		3.32 m	3.25 m	3.35 m	3.21 m	3.31 m	3.21 m	3.21 m	3.26 m	
35,35′	3.34 m		3.24 m	3.25 m		3.31 m		3.30 m		3.31 m	3.26 m	3.61 m	3.36 m	
36,36′	4.05 m		3.98 m	3.99 m		4.01 m		3.99 m		3.99 m		3.99 m	3.96 m	
	3.28 m		3.16 m	3.21 m		3.25 m		3.25 m		3.23 m		3.18 m	3.31 m	
38,38′	4.28 m	4.20 brs				4.13 m		4.27 m		4.21 m				
39,39′	3.88 m					3.70 m		3.80 m		3.81 m				
	3.66 m													
15,15′-OMe	3.34 s		3.35 s	3.35 s		3.35 s	3.33 s	3.34 s	3.32 s	3.34 s	3.32 s	3.35 s	3.36 s	3.35 s
29,29′-OMe	3.32 s		3.32 s	3.34 s		3.32 s		3.32 s		3.34 s		3.34 s		3.34 s
34,34′-OMe	3.48 s		3.56 s	3.59 s		3.47 s	3.56 s	3.48 s	3.58 s	3.48 s	3.58 s	3.55 s		
35,35′-OMe	3.44 s		3.45 s	3.45 s	3.44 s	3.43 s	3.45 s	3.44 s		3.44 s	3.45s	3.45		

[a]The data at the same atom position could be exchanged.

DOI: 10.1021/acs.joc.8b00028
J. Org. Chem. 2018, 83, 3034−3046

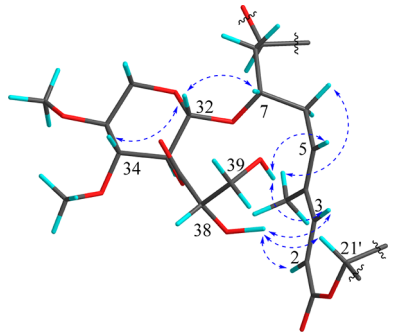

Figure 4. Key ROESY correlations of the 2,3-di-*O*-methyl-*β*-xylopyranoside and glyceryl moieties in **1** (energy minimized using standard settings for MM2 method in Chem3D 16.0).

HRESIMS analysis of samholide C (**3**) indicated its molecular formula as $C_{90}H_{152}O_{28}$, 176 mass units less than that of compound **1**, and corresponded to the absence of both glyceric acid groups. This was consistent with the presence of a monomeric quasi-molecular ion peak at *m*/*z* 863.4 in the MS/MS spectrum of **3**. The ^{1}H and ^{13}C NMR data of **3** were almost the same as those of **1**, except that the glyceric acid signals were missing and the H-33/H33′ protons were shielded by 1.5 ppm.

Samholide D (**4**) had the same molecular formula as compound **3** from HRMS data. Similar to the relationship of compounds **1** and **2**, the differences in its ^{1}H and ^{13}C NMR spectra were due to double-bond isomerization of the C-2-C-3 olefin in one-half of the dimer, as revealed by key chemical shift differences (e.g., δ_H 5.69 for H-2, δ_H 5.82 for H-2′) and twinning of many signals near this position of variance between the two monomeric halves. Thus, samholide D (**4**) was assigned as the C-2 double bond isomer of samholide C (**3**).

A molecular formula of $C_{93}H_{156}O_{31}$ was established for samholide E (**5**) from HRESIMS data, indicating that it was 88 amu less than that of compound **1**. This was consistent with the loss of one of the two glyceric acid residues from samholide A. The presence of ions at *m*/*z* 951.5 and 863.5, which result from cleavage of the two ester bonds, further indicated the loss of a glyceric acid residue from one of the two monomeric units. This change resulted again in a subtle twinning of many signals in the ^{1}H and ^{13}C NMR of **5**; for example, the H-3 and H-3′ protons of the conjugated diene differed by 0.05 ppm in chemical shift (δ_H 7.57, d, *J* = 15.55 Hz, H-3; 7.52, d, *J* = 15.56 Hz, H-3′). Thus, samholide E (**5**) was assigned a structure identical to that of samholide A (**1**) but missing one of the two glyceric acid units.

Samholides F (**6**) and G (**7**) had the same molecular formula as that of samholide E (**5**), but differed in the *Z* and *E* geometry of the C-2−C-3 double bond in either the Western or Eastern halves of the dimer. For compound **6**, there was evidence that the C-2−C-3 olefin was *Z* (δ_H 6.52, d, *J* = 12.62 Hz, H-3, and δ_H 7.44, d, *J* = 15.54 Hz, H-3′), whereas in compound **7** the C-2′-C-3′ olefin was Z (δ_H 6.46, d, *J* = 12.69 Hz, H-3′, and δ_H 7.47, d, *J* = 15.63 Hz, H-3), respectively. The sugar units, either with or without glyceric acid in the two monomeric halves of compound **6**, were determined by key ROESY correlations between H-3 and H-5 (δ_H 5.86, t, *J* = 7.00 Hz), H-5 and H-7 (δ_H 4.00, m), and H-7 and H-32 (δ_H 4.65, *J* = 6.77 Hz) (Figures S69 and S70, Supporting Information). COSY correlations between H-5/H_2-6 (δ_H 2.57, ddd, *J* = 4.06, 6.48, 13.87; 2.40, dt, *J* = 7.02, 15.36 Hz)/H-7 (Figures S63 and S64, Supporting Information), and HMBC correlations between the C-4 Me group (1.86, s) with C-3 (δ_C 148.7), C-4 (δ_C 134.7) and C-5 (δ_C 134.1), along with correlations between H-5 and C-7 (δ_C 77.0), H-7 and C-32 (δ_C 100.4), and H-32 and C-7 (Figures S65 and S66, Supporting Information), indicated that the glyceric acid residue was attached to the sugar unit located at C-7 of the 2*Z*,4*E*-monomeric structure. Further, lack of a glyceric acid residue in the 2*E*,4*E*-monomeric structure was shown by ROESY correlations between H-3′ and H-5′ (δ_H 6.14, t, *J* = 6.87 Hz), H-5′ and H-7′ (δ_H 3.97, m), and H-7′ and H-32′ (δ_H 4.39, *J* = 6.72 Hz). This was also supported by COSY correlations of H-5′/H_2-6′ (δ_H 2.69, ddd, *J* = 4.38, 6.03, 11.73; 2.28, dt, *J* = 7.45, 15.12 Hz)/H-7′, together with HMBC correlations of the C-4′ Me group protons (1.81, s) with C-3′ (δ_C 151.1), C-4′ (δ_C 134.7) and C-5′ (δ_C 138.5), the H-5′ proton with C-7′ (δ_C 75.7), the H-7′ proton with C-32′ (δ_C 102.1), and the H-32′ proton with C-7′. The combination of these NMR data thus confirmed the overall structural assignment for compound **6** as the 2*Z* double bond isomer of samholide E (**5**). Accordingly, a similar analysis for compound **7** revealed it to be the 2′*Z* double bond isomer of samholide E (**5**).

Samholide H (**8**) had a molecular formula of $C_{89}H_{150}O_{28}$ based on HRESIMS analysis. MS/MS data of **8** showed two different ions for the two monomeric halves of the molecule at *m*/*z* 863.4 and 849.4, indicating the lack of a glyceric acid residue in one-half and the lack of a methyl or methylene group in the other, relative to the monomeric structures present in compound **5**. Further, an *m*/*z* 703.3 fragment ion derived from the *m*/*z* 849.4 fragment, indicating the lack of a methyl group on the sugar residue. HSQC−TOCSY revealed the signals of both sugar units (Tables 2 and 3); however, the unit lacking the glyceric acid residue also showed an upfield shift for C-35′ (δ_C 79.3 for C-35 vs δ_C 68.9 for C-35′). Combined with the absence of this midfield methyl group signal in its ^{1}H and ^{13}C NMR spectra, it was deduced that samholide H (**8**) possessed one-half of the samholide C structure combined with a second half in which the sugar lacked the C-35 methoxy methyl group. This was further supported by COSY, HMBC, and ROESY correlation networks for these two different sugar residues (Figures S86−S93, Supporting Information).

The molecular formula of samholide I (**9**) was determined as $C_{76}H_{128}O_{20}$ from HRESIMS data. MS/MS fragmentation gave a prominent ion at *m*/*z* 703.4, suggesting that **9** was an analogue of compound **1** but lacked both the xylose sugar and glyceryl groups. Accordingly, the ^{1}H NMR spectrum of compound **9** showed no sugar or glyceric acid signals, and the 2D NMR data set was fully consistent with the aglycone structure of samholide A (**1**) (see Supporting Information).

Because the samholides (**1**−**9**) are structurally similar to the highly cytotoxic swinholides, they were evaluated for activity against the H-460 human lung carcinoma cell line. All of the samholides showed significant activity with IC_{50} values less than 1 *μ*M (Table 4), although it should be noted that these IC_{50} values are all considerably higher than those for the original swinholides.[5] However, compound **9** (samholide I), which lacks both the glyceric acid and sugar units, showed the highest IC_{50} of 0.9 *μ*M, indicating that sugar and glyceryl moieties enhance the cytotoxicity of the samholides. Compound **2** with the 2*Z* double bond, showed reduced activity compared to **1**; however, compounds **3** and **4** as well as **5** and **6**, two pairs which also differ only in the 2*E* versus 2*Z* geometry, showed equivalently high potency (0.17−0.21 *μ*M). Compound **7** with the 2′*Z* configuration, was also a highly potent compound (0.21 *μ*M). Compound **8**, which had a less methylated xylose sugar, was of lower potency in this assay. In summary, it appears that highest

DOI: 10.1021/acs.joc.8b00028
J. Org. Chem. 2018, 83, 3034−3046

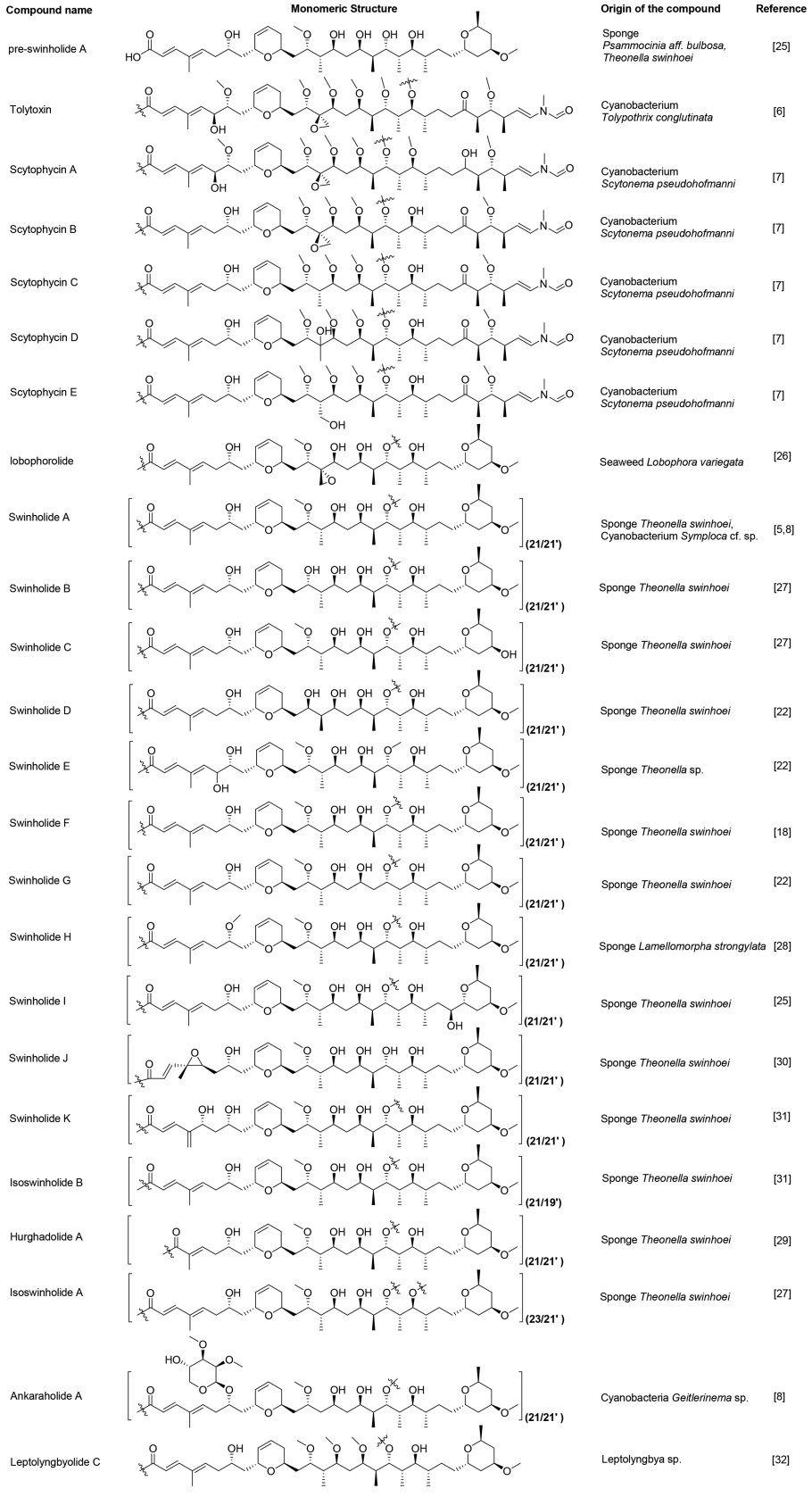

Figure 5. Monomeric structures and origins of the known swinholide-type compounds. The numbers in parentheses next to the structural diagram refer to the carbon position of dimerization.

potency among these analogs was obtained when the dimethoxylated xylose sugar was present, with or without glyceric acid residues attached.

The samholides (**1**–**9**) possess several notable structural features, including the uncommon 20-demethyl 44-membered lactone ring, methoxylated xylose sugar, and unusual glyceric acid

DOI: 10.1021/acs.joc.8b00028
J. Org. Chem. 2018, 83, 3034−3046

Table 3. ^{13}C NMR Data for Compounds 2−9 in $CDCl_3$ at 125 MHz (δ_H/δ_H' in ppm)

	2	3	4	5	6	7	8[c]	9
1/1′	167.9/170.1	170.3	167.4/169.0	170.5/169.9	167.6/169.5	169.5/167.4	170.3	169.6
2/2′	116.3/114.3	114.2	116.7/115.8	113.5/114.4	116.5/115.3	114.5/116.2	114.3/113.9	114.5
3/3′	148.6/152.2	152.4	148.5/150.5	153.1/152.1	148.7/151.1	153.9/148.3	152.2/152.1	152
4/4′	134.1	134.6	133.6	133.7/134.5	134.7	134.1	134.4	134.2
4/4′-Me	15.7/12.4	12.4	16.2/12.7	12.1/12.4	15.8/12.6	12.5/16.1	12.5/12.4	12.5
5/5′	135.0/140.6	140.8	134.8/137.9	142.7/140.3	134.1/138.5	140/134	141/134	140.3
6/6′	33.0/33.1	33.2	33.3/33.4	33.6/33.2	33	33.6/33.2	33.6/33.3	36.7
7/7′	77.4[b]/77.7[b]	76.6[b]	76.7[b]	78.6/76.6	77.0/75.7	77.2[b]/76.7[b]	76.0/76.3	69.8
8/8′	39.5/39.6	39.8	39.1	39.8/39.7	39.6/39.3	39.5/39.1	39.8/39.7	40.7[a]
9/9′	69.5	69.6	69.2/68.6	68.9/69.2	69.0/69.6	69.4/69.7	69.6	72.6
10/10′	129.7[a]/129.6[a]	129.8	129.6[a]/129.5[a]	129.7/129.8	129.6	129.5/129.6	129.8	129.4
11/11′	123.8[a]/123.7[a]	123.5	124.0/123.2	123.4/123.7	124.0/123.8	123.9/123.6	123.6	124.2
12/12′	31.5[a]/31.4[a]	31.6	31.4/31.3	31.5	31.3/31.2	31.4	31.4/31.6	31.3
13/13′	64.1/63.8	63.6	64.4/64.3	63.5/64.1	64.4/64.3	64.5	63.7/63.5	64.5
14/14′	36.2/35.9	36.9	36.1/35.7	36.2/36.7	35.7/35.6	36.1/35.9	36.9/36.8	35.9
15/15′	77.2[b]	76	78.0[b]	75.7/75.4	77.0[b]	77.0[b]	75.8/76.0	77.6[b]
15/15′-OMe	57.1[a]/57.2[a]	57.5	57.1	57.6/57.5	57.2/57.1	57.3/56.9	57.5	57.2
16/16′	41.5	41.5	41.0/41.2	41.6	40.9/40.5	40.8/40.6	41.5/41.4	40.5[a]
16/16′-Me	9.9[a]/9.6[a]	9.3	10.0/10.2	9.2/9.0	10.2/9.9	9.9	9.4/9.3	9.8
17/17′	73.9/73.6	74	73.8/74.2	73.6/73.8	74.3/74.2	74.3/74.1	74.0/74.1	7S
18/18′	40.9/41.2	40.8	41.7	40.9/40.6	41.7/41.4	41.7/41.5	40.8	40.8[a]
19/19′	69.3/68.8	69.9	69.5	70.0/69.4	69	69.8/68.3	69.8	69.2
20/20′	41.1/41.5	42.2	41.9/42.1	42.4	41.8	42.1	42.1/42.0	41.7
21/21′	71.1/71.4	70.6	71.1/70.7	70.3/70.5	71.3/70.8	70.9/71.3	70.7/70.6	70.4
22/22′	41.1/40.9	40.8	40.5	41.2/40.9	41.1/40.9	41.3/40.9	40.8/40.7	40.9[a]
22/22′-Me	10.0/10.2	10.1	10.3/10.5	9.9/10.1	10.3	10.3/10.2	10.3/10.2	10.2
23/23′	76.6/76.1	76.3	76.5	76.1/76.5	76.7	76.3	76.8[b]	76.6[b]
24/24′	33.5	33.2	33.0/32.8	33.4/33.0	33.4	33	33.2/33.3	33.3
24/24′-Me	17.6[a] /17.5[a]	17.4	17.7/17.6	17.5	17.6	17.6	17.5/17.4	17.7
25/25′	24.0[a] /23.8[a]	23.9	24.2/23.9	23.6/24.0	24	24.2/23.6	24	24.2
26/26′	29.4/29.3	29.4	29.8/29.3	29.8	29.3	29.3/29.2	29.4/29.5	29.4
27/27′	71.6/71.5	71	71.7	71.4/71.3	71.5	71.5/71.7	71.1/71.0	71.6
28/28′	35.1	35	35	35.1/35.0	35	35	35	35
29/29′	73.4	73.4	73.4	73.4	73.4	73.4	73.4	73.4
29/29′-OMe	55.4	55.4	55.4	55.4	55.4	55.4	55.5	55.5
30/30′	38.9	38.7	38.9	38.8	38.9	38.9	38.7	38.8
31/31′	64.8	64.9	64.7	64.8/64.9	64.7	64.7	64.9	64.8
31/31′-Me	22.0[a]/21.9[a]	22	22	21.9/22.0	22	21.9	21.9	22
32/32′	100.7/101.2	103.3	101.9/102.6	101.4/102.9	100.4/102.1	100.8/102.5	103.2/102.9	
33/33′	73.4	73.4	73.4	73.0/73.3	73.4/72.9	73.4/73.0	73.1/72.1	
34/34′	82.1/82.4	83.5	83.4/83.5	82.1/83.3	82.0/83.5	82.4/83.6	83.2/83.3	
34/34′-OMe	60.2[a]/60.1[a]	60.2	60.3/60.2	60.1	60.2/60.3	60.2/60.1	60.1/59.8	
35/35′	79.0/79.3	79.4	79.0/79.3	79.2	79.1	79.3	79.3/68.9	
35/35′-OMe	58.6[a]/58.7[a]	58.6	58.5	58.5	58.7[a]/58.5[a]	58.6[a]/58.5[a]	58.5/−	
36/36′	62.7	62.5	62.6	62.2/62.5	62.6	62.7	62.5/64.2	
37/37′	171.4/170.9			170.5/−	171.5/−	170.8/−		
38/38′	72.5/72.4			72.6/−	72.4/−	72.4/−		
39/39′	64.4/64.5			64.6/−	64.3/−	64.5/−		

[a]Could be exchanged. [b]Overlapped with $CDCl_3$, assigned using HMBC, HSQC, and HSQC-TOCSY. [c]The data at the same carbon atom position could be exchanged.

moiety. The previously described swinholide compounds isolated from sponges and cyanobacteria have been remarkably consistent in the structures of their fundamental carbon skeleton, and structural diversity has been observed in the side chains, position of lactonization, and overall ring size. Previous variations in methyl appendages have only been observed at positions C-16 and C-20. The glyceric acid group, generally a rare structural feature in natural products, is relatively common in cyanobacterium-derived peptides.[23] However, the occurrence of such a residue in a polyketide such as the samholides, and as a substituent on a sugar unit, is quite unique.

In 1993, Carmeli et al.[24] found that tolytoxin was a polyketide assembled from a glycine starter unit and 15 acetate repeater units, and that the one-carbon branches originated from the tetrahydrofolate C_1 pool. Recently, Ueoka et al.[11] showed that the architecture of the cyanobacterial PKS megasynthase which produces scytophycin and related compounds was highly similar to the *trans*-AT PKS cluster responsible for misakinolide production by "*Entotheonella* sp.", a symbiont in the sponge *Theonella swinhoei*. Thus, the biosynthesis of the samholides most likely follows a similar PKS pathway for construction of the carbon chains but with extra sugar and glyceric acid units attached as novel substituents.

DOI: 10.1021/acs.joc.8b00028
J. Org. Chem. 2018, 83, 3034−3046

Table 4. Cytotoxicity of Compounds 1−9 to H-460 Human Lung Carcinoma Cells[a]

compd	IC_{50}, mean ± standard errors (μM)
samholide A (**1**)	0.17 ± 0.01
samholide B (**2**)	0.52 ± 0.02
samholide C (**3**)	0.21 ± 0.08
samholide D (**4**)	0.17 ± 0.06
samholide E (**5**)	0.17 ± 0.01
samholide F (**6**)	0.17 ± 0.00
samholide G (**7**)	0.21 ± 0.01
samholide H (**8**)	0.47 ± 0.04
samholide I (**9**)	0.91 ± 0.05
doxorubicin	0.30 ± 0.02

[a]Cytotoxicity was assayed in triplicate, and doxorubicin was used as the positive control.

CONCLUSIONS

The swinholide family of compounds has attracted much attention due to their intriguing structural, biosynthetic, and pharmacological features. In the present study, nine new swinholide-related compounds, samholides A−I (**1**−**9**), were obtained from an American Samoa field collection of the cyanobacterium cf. *Phormidium* sp. (Figure 6). A 20-demethyl

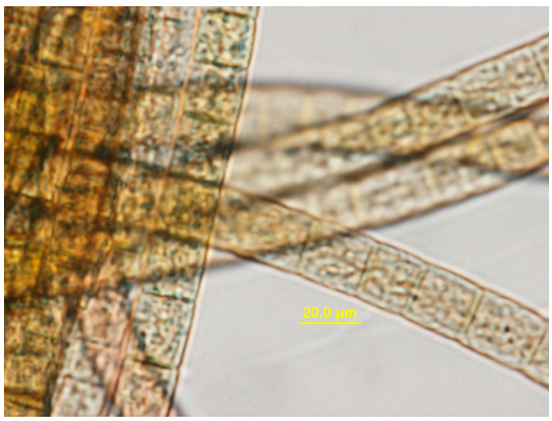

Figure 6. Photomicrograph of voucher sample of cf. *Phormidium* sp.

44-membered lactone ring distinguished these new compounds, with structural diversification occurring from geometrical isomerization of double bonds, presence of xylose sugar units with unique glyceric acid moieties, and varied *O*-methylations. The sugar and glyceric acid units appeared to enhance the relative potency of these agents in a cytotoxicity assay. Discovery of these additional representatives of the swinholide family from another cyanobacterium expands on the number of divergent species that contain this biosynthetic capacity and deepens questions concerning its evolutionary origins and history among the producing species of heterotrophic bacteria, cyanobacteria, and possibly additional sources.

EXPERIMENTAL METHODS

Optical rotation was measured on a Jasco P-2000 polarimeter. IR spectra were measured on a Thermo Electron Corp. Nicolet IR 100 FT-IR. UV/visual-light spectra were recorded on a Beckman Coulter DU 880 spectrophotometer.^{1}H NMR and 2D NMR spectra were collected on a Bruker Avance III DRX-600 NMR with a 1.7 mm dual tune TCI cryoprobe (600 and 150 MHz for ^{1}H and ^{13}C NMR, respectively). ^{13}C NMR spectra were run on a Varian X-Sens 500 MHz NMR (125 MHz) equipped with a 5 mm Xsens ^{13}C{^{1}H} cryoprobe. NMR spectra were referenced to residual solvent $CDCl_3$ signals (δ_H 7.26 ppm and δ_C 77.16 ppm as internal standards). High-resolution mass spectra were carried out on an Agilent 6230 TOF-MS under positive ion ESI-TOF-MS conditions in the University of California, San Diego (UCSD) Small Molecule MS Facility. MS fragmentation experiments were run with a Biversa Nanomate electrospray source for a Finnigan LTQ-FTICR-MS instrument running Tune Plus software version 1.0. HPLC was performed using Chromeleon 7 software with Thermo Dionex UltiMate 3000 pump and a RS diode array detector. All solvents were HPLC grade except for water, which was produced by a Millipore Milli-Q system.

Cyanobacterial Collection and Taxonomy. The marine cyanobacterium cf. *Phormidium* sp. (voucher specimen available from W. H. G. as collection no. ASX22Jul14-1) was found growing in 1.0−2.0 m of water at Fagaalu Park in American Samoa, U.S. The sample was hand collected in July 2014, preserved in a 1:1 2-propanol−seawater solution, and stored in the laboratory at −20 °C until extraction. Microscopic examination indicated that this collection was morphologically consistent with the genus *Phormidium* sp.

Extraction and Isolation. The preserved cyanobacterium was filtered through cheesecloth, and the biomass (101.7 g dry wt) was extracted repeatedly by soaking in 500 mL of 2:1 CH_2Cl_2/MeOH with warming (<30 °C) for 30 min to afford 1.8 g of dried extract. A portion of the extract was fractionated by silica gel vacuum liquid chromatography (VLC) using a stepwise gradient solvent system of increasing polarity starting from 100% hexanes to 100% MeOH [nine fractions, 100% hexanes (Fr. A, 51.7 mg), 90% hexanes/10% EtOAc (Fr. B, 132.8 mg), 80% hexanes/20% EtOAc (Fr. C 597.7 mg), 60% hexanes/40% EtOAc (Fr. D, 358.5 mg), 40% hexanes/60% EtOAc (Fr. E, 68.2 mg), 20% hexanes/80% EtOAc (Fr. F, 78.2 mg), 100% EtOAc (Fr. G, 38.6 mg), 75% EtOAc/25% MeOH (Fr. H, 180.6 mg) and 100% MeOH (Fr. I, 248.1 mg)]. Fr. I was dissolved in 50% CH_3CN/50% H_2O, subjected to chromatography on C_{18} solid-phase extraction (SPE) with a Strata 6 mL column and 1 g of C_{18}-E (55 μm, 70 Å), and eluted sequentially with 30 mL 50% CH_3CN/50% H_2O (Fr. I1, 15.2 mg), 65% CH_3CN/35% H_2O (Fr. I2, 10.4 mg), 80% CH_3CN/20% H_2O (Fr. I3, 73.2 mg), and 100% CH_3CN (Fr. I4, 15.4 mg). Fr. I2 was further purified by HPLC using a Synergi 4 μm Hydro-RP 80 Å column (10.00 × 250 mm) and isocratic elution using 97% ACN/3% H_2O at the flow rate of 3 mL/min over 45 min. This yielded six subfractions: Fr. I2A, Fr. I2B, Fr. I2C, Fr. I2D, Fr. I2E, and Fr. I2F at 13.0−16.0 min, 19.5−26.8 min, 27.2−31.0 min, 32.6−35.0 min, 36.2−38.8 min, and 41.0−44.0 min, respectively. Three fractions (Fr. I2C, Fr. I2E, and Fr. I2F) after reversed-phase HPLC were purified on the same type of column (10.00 × 250 mm Synergi 4 μm Hydro-RP 80 Å column) with different eluent solvents applied. Fr. I2C was purified using a gradient from 70% ACN/30% H_2O to 90% ACN/10% H_2O over 30 min, then 90% ACN/10% H_2O for 10 min, finally ramping back to 70% ACN/30% H_2O over 5 min, detection at 269 nm], giving compound **2** (1.4 mg) at 27.8−29.2 min. Fr. I2E was purified using 97% ACN/3% H_2O, (detection at 269 nm), giving compound **5** (5.2 mg) at 32.0−34.5 min. Fr. I2F was purified using 97% ACN/3% H_2O (detection at 269 nm) to yield **1** (5.5 mg) at 35.0−37.4 min and **3** (2.6 mg) at 39.5−42.2 min. In the same way, Fr. H was dissolved in 50% CH_3CN/50% H_2O, purified over C_{18} solid-phase extraction (SPE) with a Strata 6 mL column and 1 g of C_{18}-E (55 μm, 70 Å), and eluted sequentially with 30 mL 50% CH_3CN/50% H_2O (Fr. H1, 15.2 mg), 65% CH_3CN/35% H_2O (Fr. H2, 10.4 mg), 80% CH_3CN/20% H_2O (Fr. H3, 73.2 mg), and 100% CH_3CN (Fr. H4, 15.4 mg). Fr. H3 was separated further using RP HPLC (4 μ Phenomenex Kinetex column, isocratic 70% ACN/30% H_2O for 30 min) to yield six subfractions (Fr. H3A, Fr. H3B, Fr. H3C, Fr. H3D, Fr. H3E, and Fr. H3F at 5.6−6.7 min, 8.0−10.0 min, 10.2−14.5 min, 14.5−16.8 min, 16.8−22.0 min, and 22.5−24.5 min, respectively. Three fractions (Fr. H3B, Fr. H3C, and Fr. H3D) were further purified by RP-HPLC using a Synergi Hydro-RP 80 Å column (10.00 × 250 mm, 4 μm) or Phenomenex Luna phenyl-hexyl column with different elution solvents at a flow rate of 3 mL/min. Fr. H3B was subjected to HPLC purification with Synergi Hydro-RP 80 Å using a gradient from 88% MeOH/12% H_2O to 94% MeOH/6% H_2O over 30 min, then 94% MeOH/6% H_2O for 5 min, finally ramping back to 88% MeOH/12% H_2O over 2 min, detection at

DOI: 10.1021/acs.joc.8b00028
J. Org. Chem. 2018, 83, 3034−3046

269 nm, giving compound **8** (0.5 mg) at 29.0−31.0 min. Fr. H3C was subjected to HPLC purification using a Synergi Hydro-RP 80 Å column [isocratic 80% ACN/20% H_2O for 40 min, then a gradient from 80% ACN/20% H_2O to 90% ACN/10% H_2O over 5 min, isocratic 90% ACN/10% H_2O for 10 min, finally ramping back to 80% ACN/20% H_2O over 5 min, detection at 269 nm], giving compounds **9** (0.3 mg), **6** (0.8 mg) and **7** (0.8 mg). Fr. H3D was purified to yield compound **4** (0.3 mg) after reversed-phase HPLC using the same mobile condition.

LC−MS Analysis and Molecular Networking Generation. The crude extract and fractions A−I were dissolved in MeOH and passed through a Bond Elut-C18 OH cartridge (Agilent Technologies, USA) that was prewashed with 3 mL of CH_3CN. Subsequently, the Bond Elut-C18 OH cartridge was washed with 3 mL of CH_3CN, the solvent dried under N_2, and the residue dissolved in MeOH. A 0.020 mL aliquot of each sample was injected and analyzed via LC−MS/MS on a ThermoFinnigan Surveyor Autosampler-Plus/LC-MS/MS/PDA-Plus system coupled to a Thermo Finnigan LCQ Advantage Max mass spectrometer with a gradient of 30−100% CH_3CN in water with 0.1% formic acid. The MS/MS spectra of the crude extract and nine fractions were used to generate a molecular network following previously described methodology and visualized using Cytoscape (www.cytoscape.org).[15] Algorithms assumed a cosine threshold set at 0.7 and nodes were color-coded according to the fractions from VLC isolation.

Cytotoxicity Assay. Cytotoxicity to H-460 human lung carcinoma cells was measured as cell viability using the 3-(4,5-dimethylthiazol-2-yl)-2,5-diphenyltetrazolium bromide (MTT) reduction method.[17] Cells were cultured in Roswell Park Memorial Institute (RPMI) 1640 medium containing L-glutamine (Mediatech, Manassas, VA) and supplemented with 1 nM sodium pyruvate, 100 μg/mL streptomycin, 100 units penicillin, 0.15% sodium bicarbonate, and 10% fetal bovine serum (FBS) at 37 °C, 5% CO_2. Cells were seeded in 96-well plates at 6660 cells/well in 180 μL. After 24 h, samholides A−I (**1**−**9**) were dissolved in DMSO at 1 mg/mL. The dose−response assays used 20 uL of this DMSO stock and were diluted with 180 μL of RPMI-1640 medium (without fetal bovine serum) to 100 μg/mL followed by nine serial 25 μL:54 μL (logarithmic scale) dilutions with RPMI-1640. Subsequently, 20 μL/well of all 10 mixtures were added to cells in duplicate, resulting in a final maximal DMSO concentration of 1%. Equal volumes of RPMI-1640 medium were added to 10 wells designated as negative controls for each plate. After 48 h, the medium was removed by aspiration and cell viability determined by MTT staining. All assays were validated using doxorubicin at 1.0 and 0.1 μg/mL as the positive control. OD values were measured on ThermoElectron Multiskan Ascent plate reader at 570 and 630 nm. Dose−response graphs were generated using GraphPad Prism (GraphPad Software Inc., San Diego, CA) for IC_{50} values determination.

*Samholide A (**1**):* white amorphous solid; $[\alpha]^{27}_D$ −48 (*c* 0.1, MeOH); UV (MeOH) λ_{max} (log ε) 269 (4.72); ^{1}H NMR (600 MHz, $CDCl_3$) and ^{13}C NMR (125 MHz, $CDCl_3$) see Table 1; HRESIMS *m*/*z* 1880.0657 $[M + Na]^+$ (calcd for $C_{96}H_{160}O_{34}Na^+$, 1880.0683).

*Samholide B (**2**):* white amorphous solid; $[\alpha]^{27}_D$ −50 (*c* 0.1, MeOH); UV (MeOH) λ_{max} (log ε) 268 (4.68); ^{1}H NMR (600 MHz, $CDCl_3$) and ^{13}C NMR (125 MHz, $CDCl_3$), see Tables 2 and 3; HRESIMS *m*/*z* 1880.0654 $[M + Na]^+$ (calcd for $C_{96}H_{160}O_{34}Na^+$, 1880.0683).

*Samholide C (**3**):* white amorphous solid; $[\alpha]^{27}_D$ −52 (*c* 0.1, MeOH); UV (MeOH) λ_{max} (log ε) 269 (4.70); ^{1}H NMR (600 MHz, $CDCl_3$) and ^{13}C NMR (125 MHz, $CDCl_3$), see Tables 2 and 3; HRESIMS *m*/*z* 1704.0327 $[M + Na]^+$ (calcd for $C_{90}H_{152}O_{28}Na^+$, 1704.0362).

*Samholide D (**4**):* white amorphous solid; $[\alpha]^{27}_D$ −59 (*c* 0.1, MeOH); UV (MeOH) λ_{max} (log ε) 268 (4.66); ^{1}H NMR (600 MHz, $CDCl_3$) and ^{13}C NMR (125 MHz, $CDCl_3$), see Tables 2 and 3; HRESIMS *m*/*z* 1704.0359 $[M + Na]^+$ (calcd for $C_{90}H_{152}O_{28}Na^+$, 1704.0362).

*Samholide E (**5**):* white amorphous solid; $[\alpha]^{27}_D$ −66 (*c* 0.1, MeOH); UV (MeOH) λ_{max} (log ε) 269 (4.71); IR (neat, KBr) 3445, 3298, 2931, 1730, 1685, 1620, 1459, 1379, 1297, 1080, 1028 cm^{-1}; ^{1}H NMR (600 MHz, $CDCl_3$) and ^{13}C NMR (125 MHz, $CDCl_3$), see Tables 2 and 3; HRESIMS *m*/*z* 1792.0508 $[M + Na]^+$ (calcd for $C_{93}H_{156}O_{31}Na^+$, 1792.0523).

*Samholide F (**6**):* white amorphous solid; $[\alpha]^{27}_D$ −25 (*c* 0.1, MeOH); UV (MeOH) λ_{max} (log ε) 269 (4.69); ^{1}H NMR (600 MHz, $CDCl_3$) and ^{13}C NMR (125 MHz, $CDCl_3$), see Tables 2 and 3; HRESIMS *m*/*z* 1792.0494 $[M + Na]^+$ (calcd for $C_{93}H_{156}O_{31}Na^+$, 1792.0523).

*Samholide G (**7**):* white amorphous solid; $[\alpha]^{27}_D$ −32 (*c* 0.1, MeOH); UV (MeOH) λ_{max} (log ε) 269 (4.70); ^{1}H NMR (600 MHz, $CDCl_3$) and ^{13}C NMR (125 MHz, $CDCl_3$), see Tables 2 and 3; HRESIMS *m*/*z* 1792.0503 $[M + Na]^+$ (calcd for $C_{93}H_{156}O_{31}Na^+$, 1792.0523).

*Samholide H (**8**):* white, amorphous solid; $[\alpha]^{27}_D$ −10 (*c* 0.1, MeOH); UV (MeOH) λ_{max} (log ε) 270 (4.70); ^{1}H NMR (600 MHz, $CDCl_3$) and ^{13}C NMR (125 MHz, $CDCl_3$), see Tables 2 and 3; HRESIMS *m*/*z* 1690.0211 $[M + Na]^+$ (calcd for $C_{89}H_{150}O_{28}Na^+$, 1690.0206).

*Samholide I (**9**):* white, amorphous solid; $[\alpha]^{27}_D$ −17 (*c* 0.1, MeOH); UV (MeOH) λ_{max} (log ε) 269 (4.66); ^{1}H NMR (600 MHz, $CDCl_3$) and ^{13}C NMR (125 MHz, $CDCl_3$), see Tables 2 and 3; HRESIMS *m*/*z* 1383.8881 $[M + Na]^+$ (calcd for $C_{76}H_{128}O_{20}Na^+$, 1383.8891).

Absolute Configuration of Glyceric Acid Residue. An aliquot (0.2 mg) of compound **5** was hydrolyzed with 6 N HCl (0.3 mL) for 16 h at 90 °C. The hydrolysate was concentrated to dryness and subjected to chiral HPLC analysis (Phenomenex Chirex 3126 (D)-penicillamine (150 × 4.6 mm) HPLC column; flow rate 1 mL/min; UV detection at 254 nm; solvent 2 mM $CuSO_4$:MeOH 85:15). The retention time of glyceric acid from the hydrolyzate was 17.4 min. This was compared to authentic standards whose retention times were 14.9 min for L-glyceric acid and 17.4 min for D-glyceric acid.

■ ASSOCIATED CONTENT

Supporting Information

The Supporting Information is available free of charge on the ACS Publications website at DOI: 10.1021/acs.joc.8b00028.

Full NMR and MS data for samholides A−I (compounds **1**−**9**), NMR data comparisons with known compounds, and MS^2-based molecular network for cf. *Phormidium* sp. (PDF)

■ AUTHOR INFORMATION

Corresponding Author

*Tel: (858) 534-0578. Fax: (858) 534-0576 E-mail: wgerwick@ucsd.edu.

ORCID

Lena Gerwick: 0000-0001-6108-9000

William H. Gerwick: 0000-0003-1403-4458

Author Contributions

⊗Y.T. and P.L. contributed equally to this paper.

Notes

The authors declare no competing financial interest.

■ ACKNOWLEDGMENTS

We thank Y. Su (UCSD Chemistry and Biochemistry Mass Spectrometry Facility) for some of the HRMS data, N. Moss for help in obtaining an IR spectrum, and B. Duggan and A. Mrse for assistance with NMR technical support. This work was supported by National Institutes of Health Grant No. CA100851 (W.H.G.), Guangdong Natural Science Foundation (2016A030313588), Special Fiscal Fund of Guangdong Provincial Oceanic and Fishery Administration in 2017 (A201701607), Fund of the Education Bureau of Guangzhou City (1201610155), National Natural Science Foundation of China (Grant No. 41522605), the project of "AoShan" excellent scholar for Qingdao National Laboratory for Marine Science and Technology, and the Chinese Scholarship Council (CSC) for financial support of this work. We thank the National Fisheries and Parks Service for permits for sample collection in American Samoa.

DOI: 10.1021/acs.joc.8b00028
J. Org. Chem. 2018, 83, 3034−3046

REFERENCES

(1) Komarek, J.; Kastovsky, J.; Mares, J.; Johansen, J. R. *Preslia* **2014**, *86*, 295−335.
(2) Nunnery, J. K.; Mevers, E.; Gerwick, W. H. *Curr. Opin. Biotechnol.* **2010**, *21*, 787−793.
(3) Blunt, J. W.; Copp, B. R.; Keyzers, R. A.; Munro, M. H.; Prinsep, M. R. *Nat. Prod. Rep.* **2015**, *32*, 116−211.
(4) Mayer, A. *Marine Pharmaceuticals: The Clinical Pipeline*. http://marinepharmacology.midwestern.edu/clinPipeline.htm.
(5) Carmely, S.; Kashman, Y. *Tetrahedron Lett.* **1985**, *26*, 511−514.
(6) Moore, R. E. In *Marine Natural Products: Chemical and Biological Perspectives*; Scheuer, P. J., Ed.; Academic Press, 1981; Vol. *4*, pp 1−52.
(7) (a) Ishibashi, M.; Moore, R. E.; Patterson, G. M. L.; Xu, C.; Clardy, J. *J. Org. Chem.* **1986**, *51*, 5300−5306. (b) Moore, R. E.; Ishibashi, M.; Patterson, G. M. L.; Xu, C.; Clardy, J. *Tennen Yuki Kagobutsu Toronkai Koen Yoshishu* **1986**, *28*, 184−191. (c) Moore, R. E.; Patterson, G. M.; Mynderse, J. S.; Barchi, J.; Norton, T.; Furusawa, E.; Furusawa, S. *Pure Appl. Chem.* **1986**, *58*, 263−271.
(8) Andrianasolo, E. H.; Gross, H.; Goeger, D.; Musafija-Girt, M.; McPhail, K.; Leal, R. M.; Mooberry, S. L.; Gerwick, W. H. *Org. Lett.* **2005**, *7*, 1375−1378.
(9) Kitagawa, I.; Kobayashi, M.; Katori, T.; Yamashita, M.; Tanaka, J.; Doi, M.; Ishida, T. *J. Am. Chem. Soc.* **1990**, *112*, 3710−3712.
(10) Bewley, C. A.; Holland, N. D.; Faulkner, D. J. *Experientia* **1996**, *52*, 716−722.
(11) Ueoka, R.; Uria, A. R.; Reiter, S.; Mori, T.; Karbaum, P.; Peters, E. E.; Helfrich, E. J. N.; Morinaka, B. I.; Gugger, M.; Takeyama, H.; Matsunaga, S.; Piel, J. *Nat. Chem. Biol.* **2015**, *11*, 705−712.
(12) Humisto, A.; Jokela, J.; Liu, L.; Wahlsten, M.; Wang, H.; Permi, P.; Machado, J. P.; Antunes, A.; Fewer, D. P.; Sivonen, K. *Appl. Environ. Microbiol.* **2018**, *84*, e02321.
(13) Patterson, G. M.; Carmeli, S. *Arch. Microbiol.* **1992**, *157*, 406−410.
(14) Smith, C. D.; Carmeli, S.; Moore, R. E.; Patterson, G. M. *Cancer Res.* **1993**, *53*, 1343−1347.
(15) (a) Yeung, K.-S.; Paterson, I. *Angew. Chem., Int. Ed.* **2002**, *41*, 4632−4653. (b) Allingham, J. S.; Klenchin, V. A.; Rayment, I. *Cell. Mol. Life Sci.* **2006**, *63*, 2119−2134.
(16) Wang, M.; Carver, J. J.; Phelan, V. V.; Sanchez, L. M.; Garg, N.; Peng, Y.; Nguyen, D. D.; Watrous, J.; Kapono, C. A.; Luzzatto-Knaan, T.; Porto, C.; Bouslimani, A.; Melnik, A. V.; Meehan, Mi. J.; Liu, W.-T.; Crusemann, M.; Boudreau, P. D.; Esquenazi, E.; Sandoval-Calderon, M.; Kersten, R. D.; Pace, L. A.; Quinn, R. A.; Duncan, K. R.; Hsu, C.-C.; Floros, D. J.; Gavilan, R. G.; Kleigrewe, K.; Northen, T.; Dutton, R. J.; Parrot, D.; Carlson, E. E.; Aigle, B.; Michelsen, C. F.; Jelsbak, L.; Sohlenkamp, C.; Pevzner, P.; Edlund, A.; McLean, J.; Piel, J.; Murphy, B. T.; Gerwick, L.; Liaw, C.-C.; Yang, Y.-L.; Humpf, H.-U.; Maansson, M.; Keyzers, R. A.; Sims, A. C.; Johnson, A. R.; Sidebottom, A. M.; Sedio, B. E.; Klitgaard, A.; Larson, C. B.; Boya, C. A.; Torres-Mendoza, D.; Gonzalez, D. J.; Silva, D. B.; Marques, L. M.; Demarque, D. P.; Pociute, E.; O'Neill, E. C.; Briand, E.; Helfrich, E. J. N.; Granatosky, E. A.; Glukhov, E.; Ryffel, F.; Houson, H.; Mohimani, H.; Kharbush, J. J.; Zeng, Y.; Vorholt, J. A.; Kurita, K. L.; Charusanti, P.; McPhail, K. L.; Nielsen, K. F.; Vuong, L.; Elfeki, M.; Traxler, M. F.; Engene, N.; Koyama, N.; Vining, O. B.; Baric, R.; Silva, R. R.; Mascuch, S. J.; Tomasi, S.; Jenkins, S.; Macherla, V.; Hoffman, T.; Agarwal, V.; Williams, P. G.; Dai, J.; Neupane, R.; Gurr, J.; Rodriguez, A. M. C.; Lamsa, A.; Zhang, C.; Dorrestein, K.; Duggan, B. M.; Almaliti, J.; Allard, P.-M.; Phapale, P.; Nothias, L.-F.; Alexandrov, T.; Litaudon, M.; Wolfender, J.-L.; Kyle, J. E.; Metz, T. O.; Peryea, T.; Nguyen, D.-T.; Van Leer, D.; Shinn, P.; Jadhav, A.; Muller, R.; Waters, K. M.; Shi, W.; Liu, X.; Zhang, L.; Knight, R.; Jensen, P. R.; Palsson, B. O.; Pogliano, K.; Linington, R. G.; Gutierrez, M.; Lopes, N. P.; Gerwick, W. H.; Moore, B. S.; Dorrestein, P. C.; Bandeira, N. *Nat. Biotechnol.* **2016**, *34*, 828−837.
(17) Alley, M. C.; Scudiero, D. A.; Monks, A.; Hursey, M. L.; Czerwinski, M. J.; Fine, D. L.; Abbott, B. J.; Mayo, J. G.; Shoemaker, R. H.; Boyd, M. R. *Cancer Res.* **1988**, *48*, 589−601.
(18) Dravid, S. M.; Murray, T. F. *Brain Res.* **2004**, *1006*, 8−17.
(19) Paterson, I.; Yeung, K.-S.; Ward, R. A.; Smith, J. D.; Cuimming, J. G.; Lamboley, S. *Tetrahedron* **1995**, *51*, 9467−9486.
(20) Nicolaou, K. C.; Ajito, K.; Patron, A. P.; Khatuya, H.; Richter, P. K.; Bertinato, P. *J. Am. Chem. Soc.* **1996**, *118*, 3059−3060.
(21) Paterson, I.; Watson, C.; Yeung, K.-S.; Ward, R. A.; Wallace, P. A. *Tetrahedron* **1998**, *54*, 11955−11970.
(22) Tsukamoto, S.; Ishibashi, M.; Sasaki, T.; Kobayashi, J. *J. Chem. Soc., Perkin Trans. 1* **1991**, 3185−3188.
(23) Ishida, K.; Matsuda, H.; Murakami, M.; Yamaguchi, K. *Tennen Yuki Kagobutsu Toronkai Koen Yoshishu* **1997**, *39*, 667−672.
(24) Carmeli, S.; Moore, R. E.; Patterson, G. M. L.; Yoshida, W. Y. *Tetrahedron Lett.* **1993**, *34*, 5571−5574.
(25) Todd, J. S.; Alvi, K. A.; Crews, P. *Tetrahedron Lett.* **1992**, *33*, 441−442.
(26) Kubanek, J.; Jensen, P. R.; Keifer, P. A.; Sullards, M. C.; Collins, D. O.; Fenical, W. *Proc. Natl. Acad. Sci. U. S. A.* **2003**, *100*, 6916−6921.
(27) Kobayashi, M.; Tanaka, J.; Katori, T.; Kitagawa, I. *Chem. Pharm. Bull.* **1990**, *38*, 2960−2966.
(28) Dumdei, E. J.; Blunt, J. W.; Munro, M. H. G.; Pannell, L. K. *J. Org. Chem.* **1997**, *62*, 2636−2639.
(29) Youssef, D. T. A.; Mooberry, S. L. *J. Nat. Prod.* **2006**, *69*, 154−157.
(30) De Marino, S.; Festa, C.; D'Auria, M. V.; Cresteil, T.; Debitus, C.; Zampella, A. *Mar. Drugs* **2011**, *9*, 1133−1141.
(31) Sinisi, A.; Calcinai, B.; Cerrano, C.; Dien, H. A.; Zampella, A.; D'Amore, C.; Renga, B.; Fiorucci, S.; Taglialatela-Scafati, O. *Bioorg. Med. Chem.* **2013**, *21*, 5332−5338.
(32) Cui, J.; Morita, M.; Ohno, O.; Kimura, T.; Teruya, T.; Watanabe, T.; Suenaga, K.; Shibasaki, M. *Chem. - Eur. J.* **2017**, *23*, 8500−8509.

DOI: 10.1021/acs.joc.8b00028
J. Org. Chem. 2018, 83, 3034−3046